Am J Cancer Res 2023;13(5):1985-1998
www.ajcr.us /ISSN:2156-6976/ajcr0148915

Original Article

Low-temperature plasma-activated medium enhances the chemosensitivity of colorectal cancer cells by improving hypoxia

Yanming Xu[1,2*], Ying Li[3*], Xiaodong Yang[2], Dehua Lu[3], Yuanyuan Zheng[2], Jingyun Tan[2], Wenhua Li[3], Qi Chen[3], Yajie Liu[3], Jing Gao[2], Shubin Wang[2]

[1]Department of Clinical Medicine, Weifang Medical University, Weifang 261031, Shandong, China; [2]Department of Oncology, Shenzhen Key Laboratory of Gastrointestinal Cancer Translational Research, Cancer Institute, Peking University Shenzhen Hospital, Shenzhen-Peking University-Hong Kong University of Science and Technology Medical Center, Shenzhen 518036, Guangdong, China; [3]Department of Radiation Oncology, Peking University Shenzhen Hospital, Shenzhen 518036, Guangdong, China. [*]Equal contributors.

Received January 3, 2023; Accepted April 17, 2023; Epub May 15, 2023; Published May 30, 2023

Abstract: Studies have demonstrated that the tumour microenvironment is hypoxia and that hypoxia can induce hypoxia inducible factor-1α (HIF-1α) expression and mediate tumour chemoresistance, which leads to a very poor prognosis for cancer patients. In this study, an economical and practical HIF-1α inhibitor, plasma-activated medium (PAM), was prepared, and its role in colorectal cancer (CRC) was investigated *in vitro* and *in vivo*. We found that HIF-1α expression significantly increased under hypoxia in CRC cells followed by decreased chemosensitivity to oxaliplatin (OXA). Additionally, PAM could reduce HIF-1α expression induced by hypoxia in CRC cells, and compared to PAM or OXA alone, PAM enhanced the chemosensitivity of OXA both *in vitro* in CRC cells and *in vivo* in cell-derived xenografts, as indicated by the inhibition of cell proliferation and tumour growth. Further mechanistic studies revealed that PAM might exert synergistic antitumour activity by inhibiting the MAPK pathway, which deserves further elucidation. In summary, PAM displayed prospective clinical application due to its important function in improving hypoxia in CRC.

Keywords: PAM, hypoxia, HIF-1α, chemoresistance, colorectal cancer

Introduction

Although treatment strategies and early screening are becoming more prevalent, the morbidity and mortality of colorectal cancer (CRC) are still very high worldwide, requiring urgent treatment methods [1]. For most CRC patients, drug-based comprehensive therapy is the main method, of which chemotherapy plays an indispensable role. However, due to insufficient vascularization inside solid tumours, tumour cells are often in a hypoxia and low pH state, which can ultimately induce chemoresistance by changing the expression of molecules [2-4]. Currently, hypoxia-mediated chemoresistance is still difficult to resolve in most cancers, including CRC.

Hypoxia inducible factor-1α (HIF-1α) is a critical hypoxia molecule. HIF-1α is hydroxylated by proline hydroxylases (PHDs) followed by recognition of the e3 ubiquitin ligase complex, which subsequently leads to its degradation under normoxic conditions [5]. However, when tumour cells are hypoxia, chemoresistance is promoted by a cascade of processes inside cells, including inactive PHDs, HIF-1α subunit translocation into the nucleus, and changes in gene transcription and protein expression [6, 7]. Minassian, L.M. et al. demonstrated that HIF-1α overexpression reduced tumour senescence and induced therapeutic resistance in tumour cells [8]. Mohsen Rashid et al. revealed that HIF-1α could mediate chemoresistance by multiple mechanisms [9]. Therefore, targeting HIF-1α by physical or chemical means is expected to overcome chemoresistance in cancer patients.

Plasma is widely present in nature and is considered to be the fourth material state other

than solid, liquid, and gaseous states. Thermal plasma is commonly generated by lightning, but it is not suitable for medical applications due to heat. Therefore, low-temperature plasma technology operating at atmospheric pressure and room temperature has been developed [10]. In recent years, low-temperature plasma technology has been deeply studied in various mammalian cells and is expected to be an emerging technology for the treatment of cancers [11]. Plasma-activated medium (PAM) was prepared using a low-temperature plasma device, and the proliferation of cancer cells could be inhibited when cultured with PAM [12, 13]. PAM might display a promising application similar to photodynamic therapy. In our previous study, PAM treatment significantly reduced cell viability and inhibited the formation of multicellular spheres in lung cancer cells [12]. Further research has shown that PAM can inhibit the phosphorylation of ERK and P38, followed by degradation of HIF-1α and increased chemotherapy sensitivity [14-17].

Based on a previous study, this study was first designed to explore the role of PAM in CRC *in vitro* and *in vivo*. We found that hypoxia CRC cells stably expressed HIF-1α and showed chemoresistance to oxaliplatin (OXA). PAM could inhibit HIF-1α expression and enhance OXA sensitivity in CRC cells and xenografts by inhibiting the MAPK pathway, which should be further investigated in the future to provide a new auxiliary method for CRC treatment.

Materials and methods

Cell culture

Human CRC cell lines (HCT8, HT29 and HCT116) were obtained from our preserved cell banks and cultured in Dulbecco's modified Eagle's medium (DMEM, Viva cell) supplemented with 10% foetal bovine serum (FBS, Gibco, USA), 1% penicillin streptomycin (P/S, Gibco, USA) and 1% nonessential amino acid X 100 (NEAA x100, Gibco, USA). Aerobic cells were routinely cultured in a humidified incubator containing 5% CO_2 at 37°C. Hypoxia cells were cultured in 1% O_2 according to a previously reported study [18].

Preparation of PAM and detection of ROS and RNS

The plasma device used in this study is shown in **Figure 2A** and **2B**, which mainly includes an electrode, DC power supply, probe, and gas pipe. The internal electrode with a resistance of 500 MΩ is externally connected to a DC power supply of 4.7 KV at one end and a probe of 50 μm at another end. Helium and oxygen enter the gas pipe at 2 mL per minute and 10 mL per minute, respectively. When connecting the power supply, the probe produces a low-temperature plasma flow (i.e., mauve flame) after contacting helium and oxygen. An Eppendorf tube with a volume of 1.5 mL was used to prepare the PAM in our study, and the injection port of the plasma device was flush with the upper edge of the 1.5 mL Eppendorf tube. ROS (reactive oxygen species) and RNS (reactive nitrogen species) levels in PAMs were detected with H_2O_2 and NO_X assay kits (BioAssay Systems, USA) according to the manufacturer's instructions.

Cell viability assay

CRC cells were inoculated into 96-well plates at 5000 cells/well, and the cells were allowed to attach overnight. Cells were treated with OXA (concentrations of 0, 0.0005, 0.005, 0.05, 0.5, 5, 50, and 500 μg/mL) or PAM for different activation times (0, 4, 8, 12, 16, and 20 min). The treated cells were cultured under normoxic and hypoxic conditions for 12 h and then transferred to normoxic conditions for another 36 h. Cell viability was evaluated using Cell Counting Kit-8 (Beyotime, China) reagent according to the manufacturer's instructions. The OD value was measured with a spectrophotometer (Thermo Fisher, USA) at 450 nm absorbance followed by calculation with ImageJ software.

Live/dead cell assay

CRC cells at a cell density of 5×10^4 cells/well were inoculated into 24-well plates and incubated overnight followed by PAM treatment. Cells were washed with phosphate-buffered saline (PBS) and then stained according to the instructions of the calcein-AM/PI double staining kit (Yeasen, Shanghai, China). Briefly, 500 μL of 1X buffer, 0.5 μL calcein-AM, and 1.5 μL PI (propidium iodide, PI) were added to each well and incubated at 37°C for 15 min, and then the cells were observed and photographed under a fluorescence microscope (Leica, Germany).

TUNEL staining

CRC cells were seeded into 24-well plates with round cell slides at a density of 10^4 cells/well.

After applying different treatments, TUNEL staining was performed on slides containing cells according to the instructions of the ApopTagRFluorescein in situ apoptosis detection kit (Millipore, Germany). After fixing the slides, the slides were observed and photographed under a confocal microscope (Leica, Germany).

Colony formation assay

CRC cells were inoculated into 6-well plates at a density of 600 cells/well and incubated for 24 hours. Cells were initially treated with PAM, OXA and PAM+OXA under anoxic conditions for 12 h, and then cells were cultured under normal oxygen conditions for 12 days. After a series of operations, including PBS (Gibco, USA) washing, 4% paraformaldehyde (Beyotime, China) fixation, and crystal violet staining, cell pictures were taken using an ultrasensitive imaging system (Amersham ImageQuant 800, Cytiva, USA). Data were analysed using ImageJ software.

Western blot

Cells were harvested and lysed using appropriate amounts of lysates containing RIPA buffer (Sangon Biotech, China), protease inhibitors (Zhonghui Hercai, China), and PMSF (Zhonghui Hercai, China), and protein concentrations were detected using a BCA protein assay kit (Sangon Biotech, China). Approximately 30 μg of protein samples were separated on a 12% SDS-PAGE gel and subsequently transferred to PVDF membranes (Millipore, MA, USA). Membranes were blocked with 5% bovine serum albumin (BSA) for 1 h at room temperature followed by incubation with primary antibodies against HIF-1α (Cell Signaling Technology, 36169, 1:1000), p-ERK (Cell Signaling Technology, USA, 9101S, 1:1000), ERK (Cell Signaling Technology, USA, 9102S, 1:1000), p-P38 (Cell Signaling Technology, USA, 9211S, 1:1000), P38 (Cell Signaling Technology, USA, 9212S, 1:1000), and GAPDH (Proteintech, USA, 10494-1-AP, 1:5000) at 4°C overnight and secondary antibody (HRP conjugated anti-rabbit IgG, Cell Signaling Technology, USA, 7074S, 1:5000) at room temperature for 1 h. Finally, proteins were detected using chemiluminescence solution (Beyotime Institute of Biotechnology, China) and imaged on an ultrasensitive imaging system (Amersham ImageQuant 800, Cytiva, USA).

Animal experiments

All animal experiments in this study were performed according to the guidelines of the Animal Research Committee of Peking University Shenzhen Hospital. Six-week-old female Balb/c nude mice (GemPharmatech Company, Guangdong, China) were used to establish subcutaneous xenografts by injection of 1×10^6 HT29 cells/mouse. When xenografts reached approximately 100 mm^3, mice were randomized into various groups (CTRL, PAM, HIF-1α inhibitor PX-478, OXA, PX-478+OXA, and PAM+OXA; ≥ 4 mice per group). PAM or drug administration was as follows: $PAM^{20\ min}$ (intratumoral injection, twice weekly for 3 weeks), 10 mg/kg of OXA (intraperitoneal injection, twice weekly for 3 weeks), and 20 mg/kg of PX-478 (intraperitoneal injection, twice weekly for 3 weeks). Tumour size and weight were measured twice weekly, and tumour volume and tumour growth inhibition (TGI) were calculated using the following formulas: volume = 1/2 × (length of long diameter) × (width of short diameter)^2; TGI = [1-(ΔT/ΔC)] × 100% (ΔT and ΔC presented tumour volume changes of treatment group and control group on the last day compared to initial administration, respectively).

H&E and immunohistochemical staining

At the end of animal experiments, xenografts and organs (heart, liver, spleen, lung and kidney) were collected and prepared into paraffin sections approximately 4 μm in thickness. Haematoxylin and eosin (H&E) staining was performed according to the methods in relevant studies [19]. For immunohistochemical (IHC) staining of xenografts to evaluate HIF-1α and Ki67 expression, primary antibodies against HIF-1α (Cell Signaling Technology, USA, 36169, 1:200) and Ki67 (Abcam, UK, ab1667, 1:200) were used in this study. The IHC procedures were performed according to a previously reported study [20]. Briefly, after a series of operations containing deparaffinization, hydration, antigen retrieval, endogenous peroxidase removal, BSA blocking, primary antibody incubation, and secondary antibody incubation, the sections were finally stained with DAB chromogenic solution followed by the evaluation of

expression based on a reported method [21] and analysed by ImageJ software.

Transcriptome sequencing

Total RNA of xenografts was extracted using TRIzol reagent (Invitrogen, Cat. No. 15596-018) followed by measurement of RNA concentration with a NanoDrop 2000 Ultramicrospectrophotometer (Thermo Fisher, USA). After preparation of the mRNA library, transcriptome sequencing was performed using an Illumina NovaSeq 6000 sequencer (Illumina, USA) at Chi Biotech Co., Ltd, Shenzhen, China. Data quantitative analysis was performed using featureCountsv2.0.1 software, and differential expression analysis was performed using edgeRv3.28.1. Genes with log2 (fold change) > 1 were defined as upregulated genes, and genes with log2 (fold change) < 1 were defined as downregulated genes. GO and KEGG enrichment analyses of differentially expressed genes were performed using topGOv2.38.1 and clusterProfilerv3.14.3 software, respectively.

Statistical analysis

Data are represented by the means ± standard deviations of replicate sets (at least three times). GraphPad Prism version 8.00 (GraphPad Software, USA) was used to analyse the data. Student's t test was used to evaluate significance between groups. Fisher's exact test and hypergeometric test were used to analyse GO and KEGG enrichment results. The statistically significant differences were described as $^{*}P < 0.05$, $^{**}P < 0.01$, and $^{***}P < 0.001$.

Results

Hypoxia induced high HIF-1α expression and chemoresistance in CRC cells

CRC cell lines were cultured under hypoxia for different times (0, 1, 4, 8, 12, and 24 h), and HIF-1α expression was induced with expression peaks at 4-12 h of hypoxia and then gradually decreased (**Figure 1A** and **1B**), which suggested the successful establishment of hypoxic cell models. In the following study, hypoxic cells were used after culture under hypoxia for 12 h. As expected, compared to normoxic cells, hypoxic cells displayed OXA chemoresistance, as indicated by higher IC50 values (HCT8 cells: 25.18 ng/μL vs. 7.78 ng/μL; HCT116 cells: 9.12 ng/μL vs. 2.05 ng/μL; HT29 cells: 15.19 ng/μL vs. 3.25 ng/μL), as shown in **Figure 1C** and **1D**.

The preparation of PAM and identification by contents of H_2O_2 and NO_X

In this study, PAM with different plasma exposure times (4, 8, 12, 16 and 20 min) named PAM^{Xmin} was prepared using the device shown in **Figure 2A** and **2B**, followed by the detection of H_2O_2 and NO_X contents in PAM. The results showed that the contents of H_2O_2 and NO_X in PAMs increased with prolonged plasma exposure time (**Figure 2C** and **2D**). Considering that H_2O_2 and NO_X are consumed at ambient atmospheric pressure, CRC cells treated with PAM were cultured for 12 h, and supernatants were collected to measure the contents of H_2O_2 and NO_X. As shown in **Figure 2E** and **2F**, although the contents of H_2O_2 and NO_X decreased slightly, they remained relatively high compared to freshly prepared PAM, suggesting the potential application prospects of PAM in the future.

PAM inhibited cell viability by decreasing hypoxia-induced HIF-1α expression

As expected, PAM inhibited cell viability both in hypoxic CRC cells (**Figure 3A**) and in normoxic CRC cells (Figure S1A) in a plasma exposure time-dependent manner, suggesting its potential antitumour activity. To observe the sensitization effect of PAM to chemotherapy drugs, $PAM^{12\ min}$ was used in the following *in vitro* study. Compared to the control, PAM treatment significantly induced more cell death in hypoxic CRC cells (HCT8 cells: 0.11 vs. 0.02; HCT116 cells: 0.12 vs. 0.02; HT29 cells: 0.22 vs. 0.05; **Figure 3B** and **3C**), as well as in normoxic cells (HCT8 cells: 0.08 vs. 0.006; HCT116 cells: 0.10 vs. 0.004; HT29 cells: 0.19 vs. 0.02; Figure S1B and S1C). The TUNEL assay confirmed that PAM induced more cell apoptosis than the control in both hypoxic (HCT8 cells: 4.47 vs. 1.0; HCT116 cells: 3.7 vs. 0.7; HT29 cells: 4.0 vs. 1.3; **Figure 3D**) and normoxic CRC cells (HCT8 cells: 3.3 vs. 0.3; HCT116 cells: 3.3 vs. 0.4; HT29 cells: 3.4 vs. 0.3; Figure S1D). Next, proteins were extracted from cells under hypoxia or normoxic conditions with or without PAM treatment according to the flows of **Figure 3E1**, followed by western blot detection. The results showed that PAM^{12min} could effectively decrease hypoxia-induced HIF-1α expression (**Figure 3E2**).

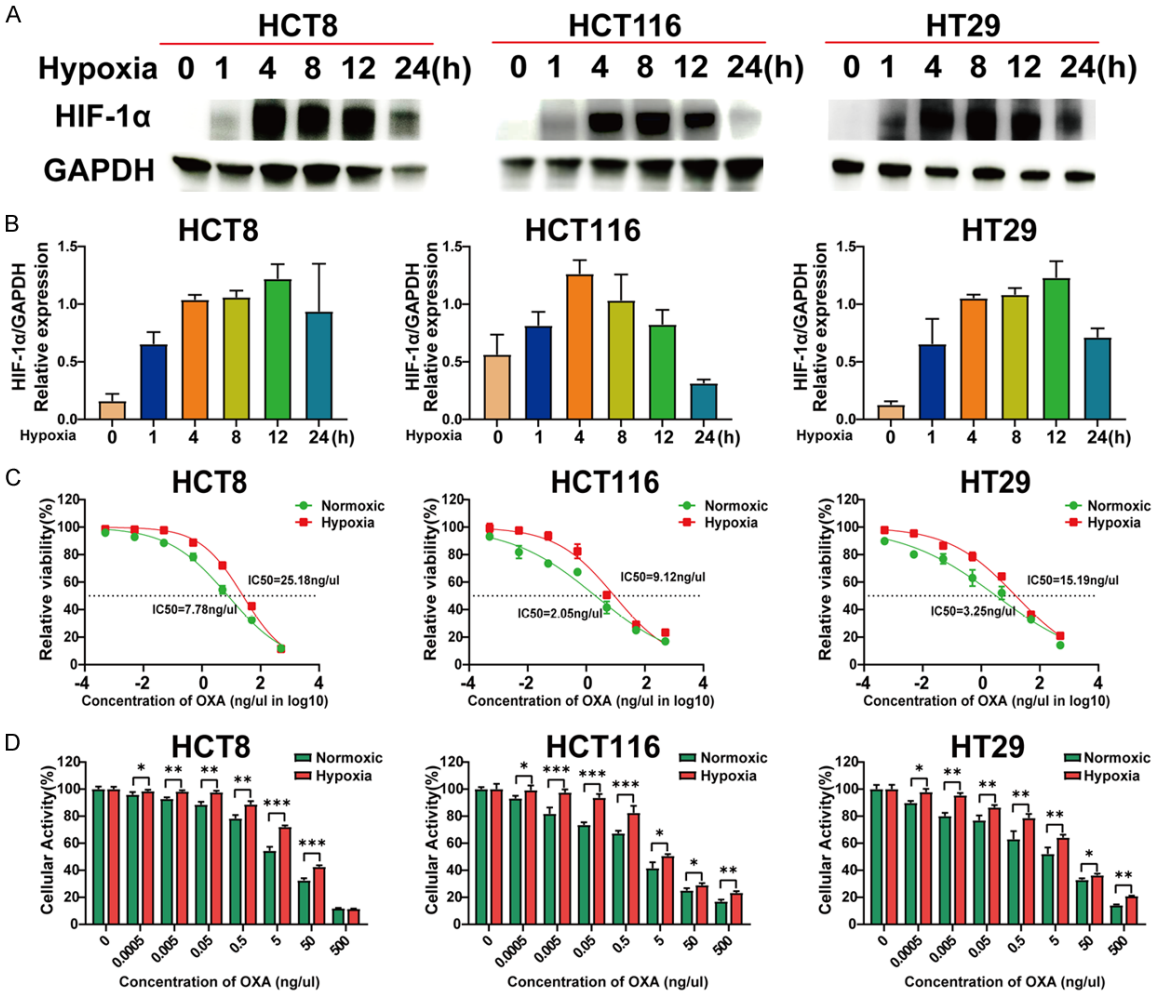

Figure 1. Hypoxia induced high HIF-1α expression and chemoresistance to OXA in CRC cells. (A) HIF-1α expression was increased gradually under hypoxia with a peak at 4-12 h by western blot analysis. GAPDH was used as the endogenous control. (B) The quantification of HIF-1α/GAPDH based on the results of (A) performed by ImageJ. (C) Cell viability curve after treatment with OXA at different concentrations. The calculated IC50 value under hypoxia or normoxia was also annotated. (D) Quantitative histogram of cell viability treated with different concentrations of OXA under hypoxia or normoxia. The results are presented as the mean ± standard deviation of three independent experiments. $^{*}P < 0.05$, $^{**}P < 0.01$, $^{***}P < 0.001$.

PAM enhanced the chemosensitivity of hypoxic CRC cells to OXA in vitro

Hypoxic CRC cells were treated with PAM alone, OXA alone or PAM combined with OXA, and cell viability assays revealed that PAM or OXA alone exerted similar inhibitory effects, while PAM combined with OXA displayed significant synergistic cell inhibition, suggesting the enhanced chemosensitivity of PAM to OXA (**Figure 4A**). Additionally, the numbers of cell colonies (**Figure 4B** and **4C**) were obviously decreased in the PAM combined with OXA group, as well as the corresponding increased cell death in the combined group (**Figure 4D**). The TUNEL assay also confirmed that PAM combined with OXA induced more cell apoptosis than the other treatments (**Figure 4E**). All these results suggested that PAM enhanced OXA sensitivity *in* hypoxic CRC cells *in vitro*, which was validated *in vivo*.

PAM combined with OXA exerted strong synergistic tumour suppression in vivo

Mouse models bearing HT29 cell-derived subcutaneous xenografts were used in this study, and the HIF-1α inhibitor PX-478 was used as a positive control [22]. The mice in the 6 groups were treated according to the scheme shown in

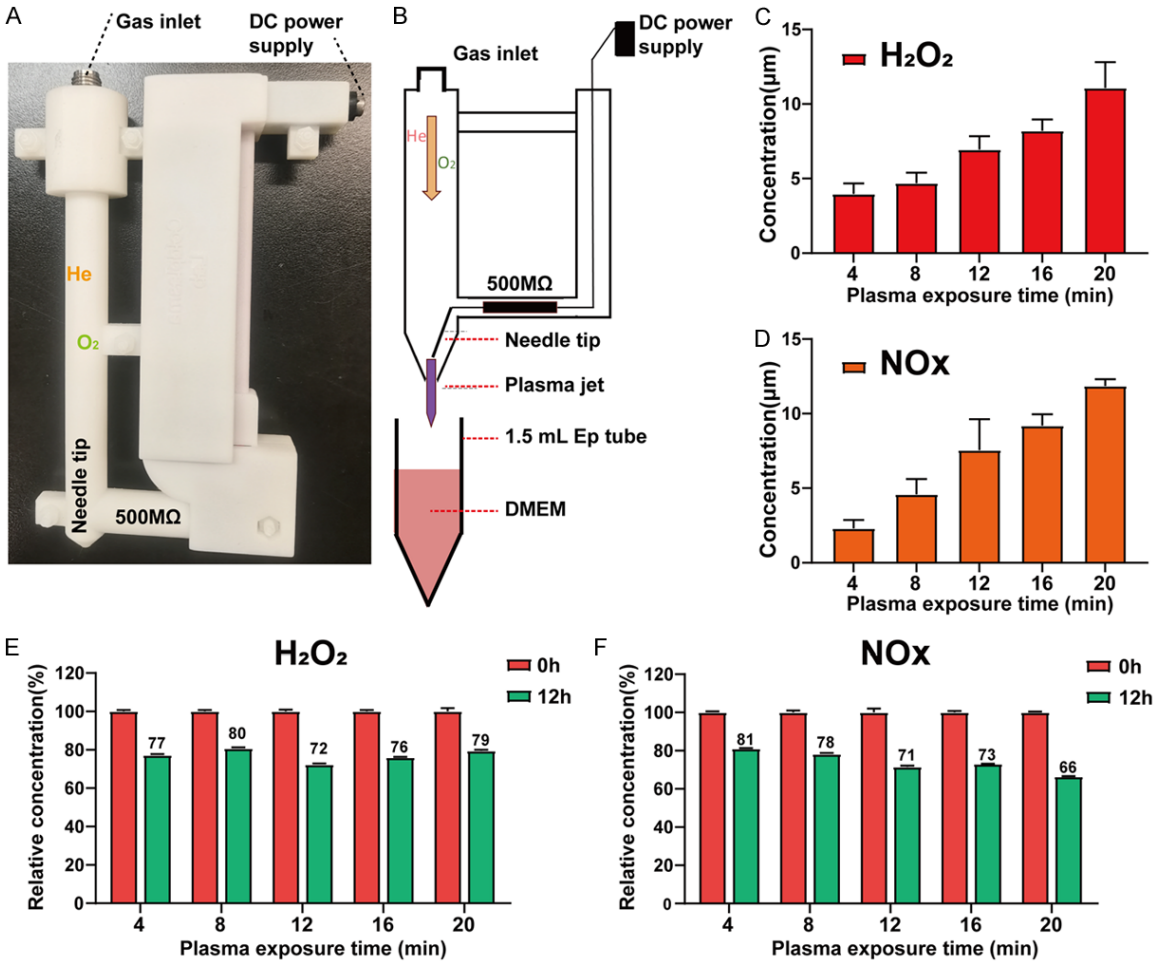

Figure 2. PAM preparation device and evaluation of the contents of H_2O_2 and NO_x. (A) Picture of the PAM preparation device in our study. (B) Schematic drawing of the PAM device with internal and external instruction presentation. (C) H_2O_2 and (D) NO_x contents in prepared PAMs with different plasma exposure times. (E) H_2O_2 and (F) NO_x consumption after cells were cultured in PAM for 12 h. Compared to freshly prepared PAM, the contents of H_2O_2 and NO_x in PAM after 12 h of culture decreased slightly. The results are presented as the mean ± standard deviation of three independent experiments.

Figure 5A. From **Figure 5B** and **5C**, we found that compared to other groups, PAM combined with OXA exerted strong and identical suppressive activity to PX-478 combined with OXA against CRC xenografts indicated as high TGI (75.0% in PAM+OXA group, 74.1% in PX-478+OXA group) and light tumour weight (0.28 g in PAM+OXA group, 0.27 g in PX-478+OXA group). Although the mouse weight in the combined treatment groups showed a slight decrease (**Figure 5B**), the loss of body weight was most likely caused by OXA rather than PAM or PX-478, suggesting the potential good tolerance of PAM, as well as its nontoxicity (**Figure 5D**). HIF-1α and Ki67 of xenografts at the end of experiments were stained, and the results demonstrated that HIF-1α was significantly inhibited by PX-478 or PAM rather than OXA, and cell proliferation was obviously suppressed by either combination therapy, as indicated by very weak staining of Ki67 (**Figure 5E**).

The MAPK/ERK pathway might be involved in the PAM-induced HIF-1α decrease

To elucidate the potential mechanisms involved in PAM activity, xenografts treated with CTRL, PAM alone, OXA alone, and PAM+OXA were subjected to transcriptome sequencing. A total of 248 differentially expressed genes (DEGs) were identified in PAM-treated xenografts compared with the control group, with 61 upregu-

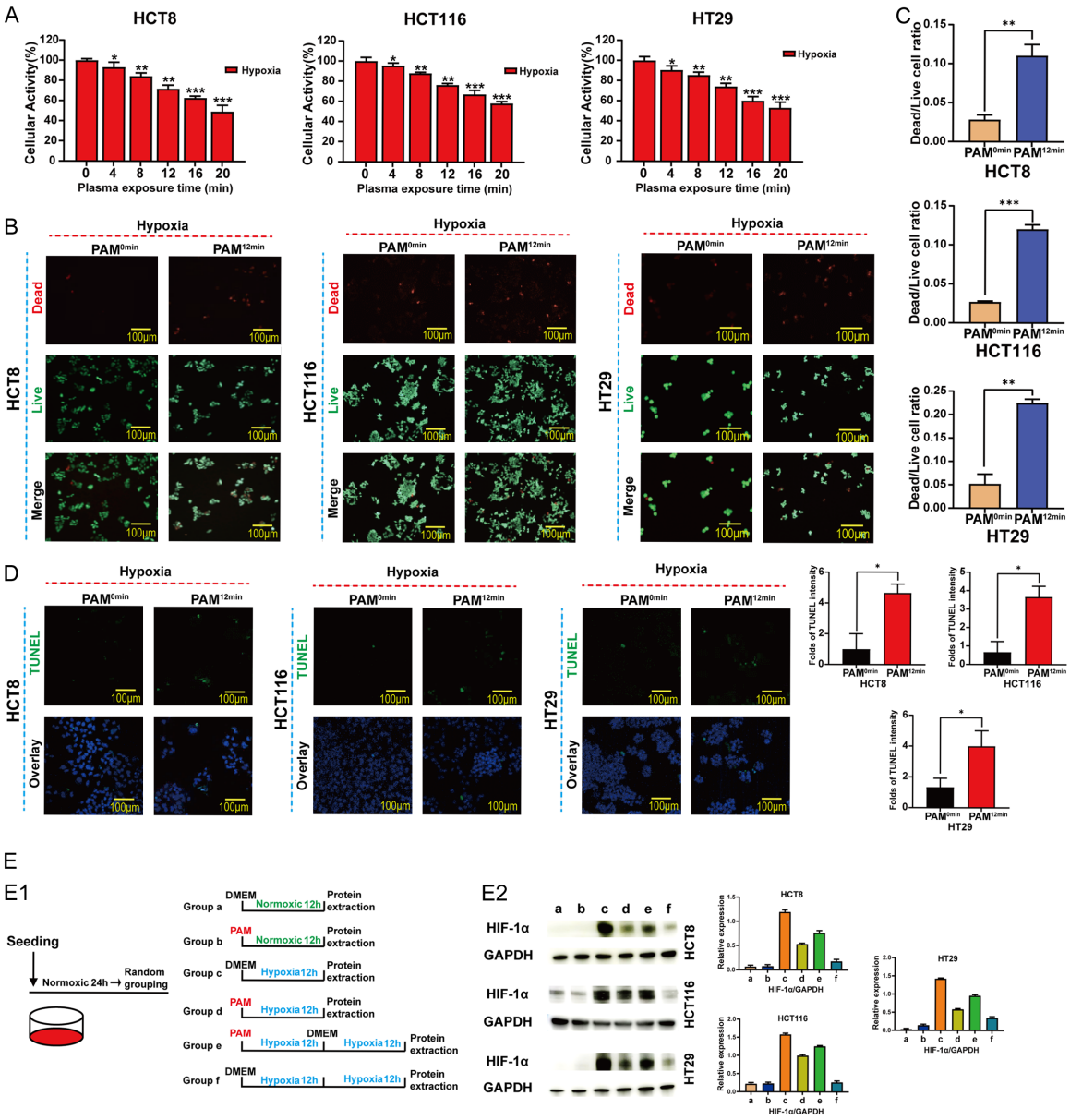

Figure 3. PAM inhibited cell viability by decreasing hypoxia-induced HIF-1α expression. (A) Hypoxic CRC cells could be inhibited by PAM in a plasma exposure time-dependent manner. (B) The staining results of live/dead cells treated with or without PAM. Red represents dead cells, and green represents live cells. (C) Quantification of the dead/live cell ratio in CRC cells treated with or without PAM. (D) The percentage of cell apoptosis was increased by PAM in hypoxic CRC cells evaluated by TUNEL assay. (E1) Schematic diagram of CRC cells cultured under different conditions with or without PAM. (E2) HIF-1α expression in different groups of (E) was detected by western blot, and quantification of HIF-1α/GAPDH was performed by ImageJ. GAPDH was used as an endogenous control. The results are presented as the mean ± standard deviation of three independent experiments. $^{*}P < 0.05$, $^{**}P < 0.01$, $^{***}P < 0.001$.

lated genes and 187 downregulated genes. Moreover, compared to OXA-treated xenografts, 381 DEGs were identified in PAM+OXA tumours, with 315 upregulated genes and 66 downregulated genes (**Figure 6A**). Therefore, Gene Ontology (GO) and Kyoto Encyclopedia of Genes and Genomes (KEGG) pathway enrichment analyses were performed, and the mitogen-activated protein kinase (MAPK) pathway was mainly enriched in the GO analysis (**Figure 6B**) and KEGG analysis (**Figure 6C**). Based on reported studies [14, 15], the critical molecule of ERK was evaluated by western blot, and the expression of phosphorylated ERK (p-ERK) was decreased in the PAM or PAM+OXA groups rather than total ERK (**Figure 6D**), as well as

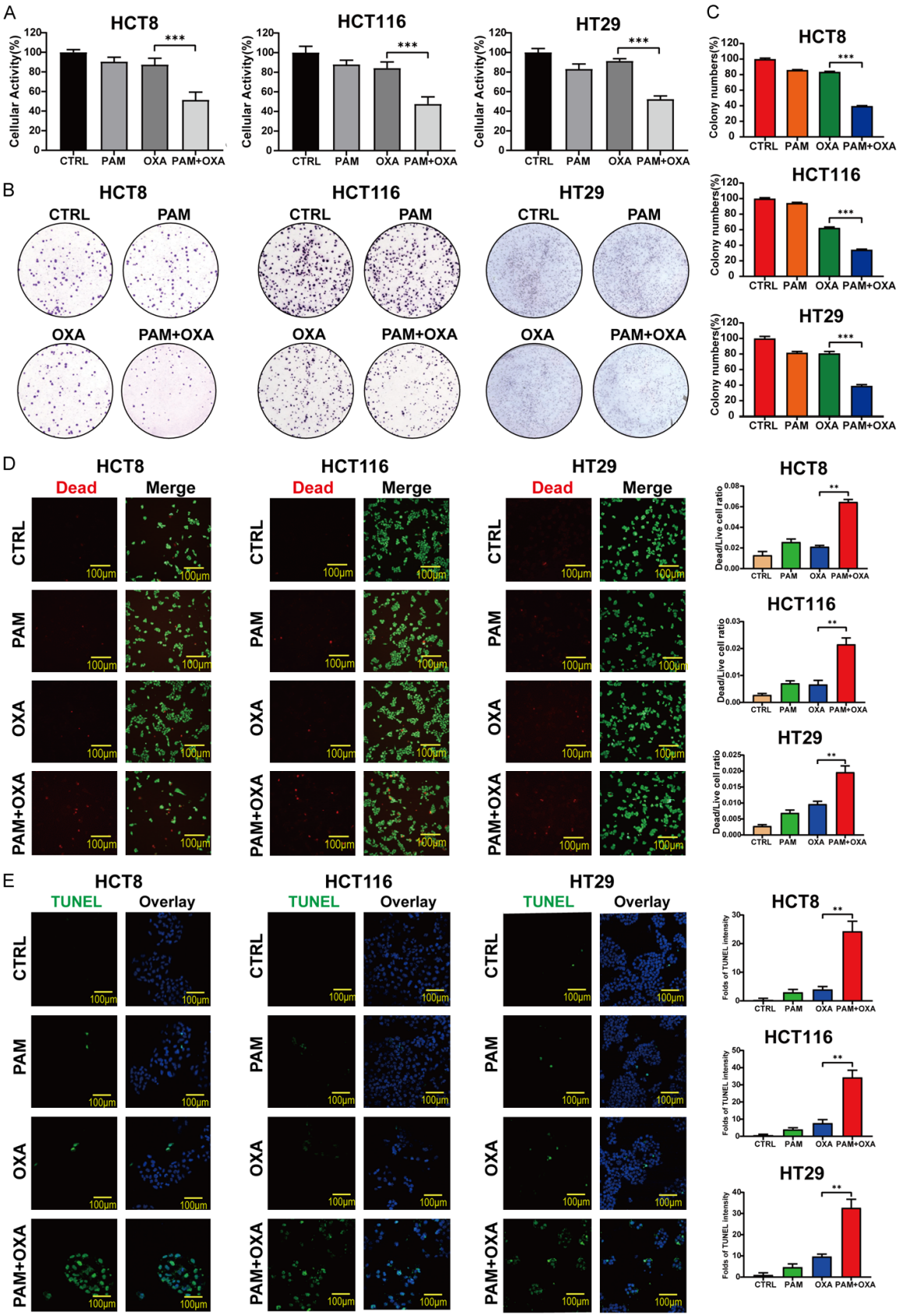

Figure 4. PAM enhanced the sensitivity of OXA in hypoxic CRC cells *in vitro*. (A) Cell viability of hypoxic CRC cells after treatment with CTRL, PAM, OXA, and PAM+OXA. (B) Pictures and (C) quantitative histograms of colonies evaluated

by colony formation assay in different treatment groups. (D) PAM combined with OXA induced more dead cells than other groups indicated as red. Green represents live cells. (E) The percentage of cell apoptosis was higher in the PAM+OXA group than in the other groups, as evaluated by TUNEL assay. The results are presented as the mean ± standard deviation of three independent experiments. $^{*}P < 0.05$, $^{**}P < 0.01$, $^{***}P < 0.001$.

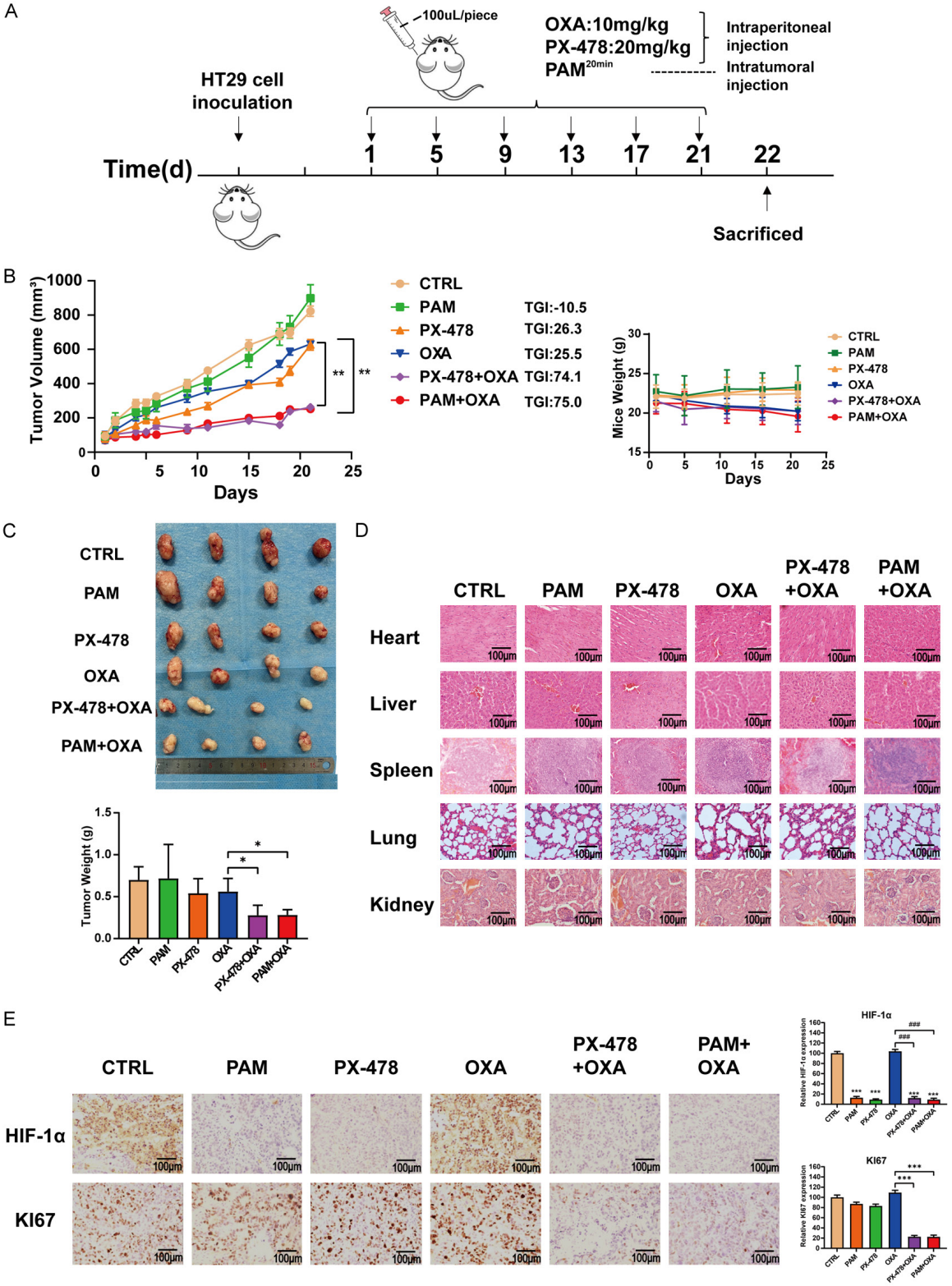

Figure 5. PAM combined with OXA exerted strong synergistic tumour suppression in CRC xenografts. A. Schematic diagram of mice receiving different treatments. B. Tumour growth curve of mice indicated the highest inhibition in groups of OXA combined with PAM or PX-478, and changes in mouse body weight during the treatment. C. Tumour pictures at the end of experiments and tumour weight was measured. D. No obvious toxicity was found in the heart, liver, spleen, lung and kidney of mice based on H&E staining. E. HIF-1α and Ki67 expression was evaluated in xenografts receiving different treatments. The scale was 100 μm. The results are presented as the mean ± standard deviation of three independent experiments. $^{*(\#)}P < 0.05$, $^{**(\#\#)}P < 0.01$, $^{***(\#\#\#)}P < 0.001$.

decreased HIF-1α. Meanwhile, the MAPK/P38 pathway is also inhibited by PAM (Figure S2), which will be further investigated in the future.

Discussion

Hypoxia is a frequent event in solid tumours, and HIF-1α expression has been verified to be a hallmark of hypoxia, which is closely correlated with chemoresistance and urgently needs to be resolved [23]. HIF-1α expression first increased and then gradually decreased under hypoxia in our study, which was also found in other studies [24, 25]. Therefore, we established hypoxia cell models by culturing cells for 12 h under hypoxia and confirmed that hypoxia cells developed chemoresistance to OXA compared to normoxic cells, as indicated by a higher IC50 value. Consistent with other reports [26], these results suggested that hypoxia induced increased expression of HIF-1α, which contributed to a decreased sensitivity of CRC cells to OXA. For chemotherapeutics of CRC in clinical practice, oxaliplatin, 5-Fu, and irinotecan are the most commonly used drugs [27]. As described above, only OXA was used in this study, and we suspected similar results for the other CRC chemotherapy drugs because hypoxia-induced chemoresistance was not limited by drug classification, which will be further validated in our ongoing studies.

In recent years, PAM has been widely used in the field of biological medicine, especially in cancer research, and “plasma oncology” has emerged [28, 29]. PAM has been reported to play an important role in cancer suppression for a variety of cancers [30]; however, most of these studies were conducted in normoxic cancer cells. Hypoxia is a critical feature of malignant tumours, and cancer cells obtain energy through glycolysis by accelerating cell growth under hypoxia, which can also quickly contribute to drug resistance [31]. Therefore, it is necessary to explore the role of PAM in overcoming drug resistance by improving hypoxia. In our study, PAM with different plasma exposure times was prepared using a special device, and its inhibitory effect on both normoxic and hypoxia CRC was confirmed both *in vitro* and *in vivo* by approving hypoxia, especially its sensitization effect on chemotherapy drugs. HT29 cell-derived subcutaneous xenografts in mice were used, and PAM was administered by intratumoral injection in this study, which was different from clinical practice. Cell- or patient-derived orthotopic xenografts in the colorectum are the optimal choice for preclinical studies [32, 33] and should be established to validate the efficacy of PAM. Additionally, similar to photodynamic therapy [34, 35], PAM administered through the intestinal tract by special equipment such as endoscopes might be an alternative strategy in the real world.

Because of insufficient vascularization inside solid tumours, tumour cells are often in a hypoxia state, which was confirmed in our study. Based on **Figure 1**, CRC cells cultured in two dimensions *in vitro* without hypoxia did not express HIF-1α; however, HIF-1α was highly expressed in solid xenografts derived from cells (**Figure 5**). Although angiogenesis was not detected in our study, high expression of HIF-1α in xenografts suggested hypoxia inside the xenografts, which also demonstrated that hypoxia could be approved by intratumoral injection of PAM. In addition to the sensitization effect of PAM, the toxicity of PAM was also considered. From **Figure 5**, the mouse weights in the combined treatment groups and OXA group showed a slight identical decrease, which suggested no extra toxicity induced by PAM or PX-478. Additionally, no abnormal changes were found in critical organs of mice treated with PAM, indicating the safety of PAM and its potential application.

Hypoxia induces chemoresistance by increasing HIF-1α expression, but the underlying regulatory mechanisms are unclear. To provide useful clues for further investigation, transcriptomic sequencing of some xenografts treated with PAM was performed. GO analysis emphasizes

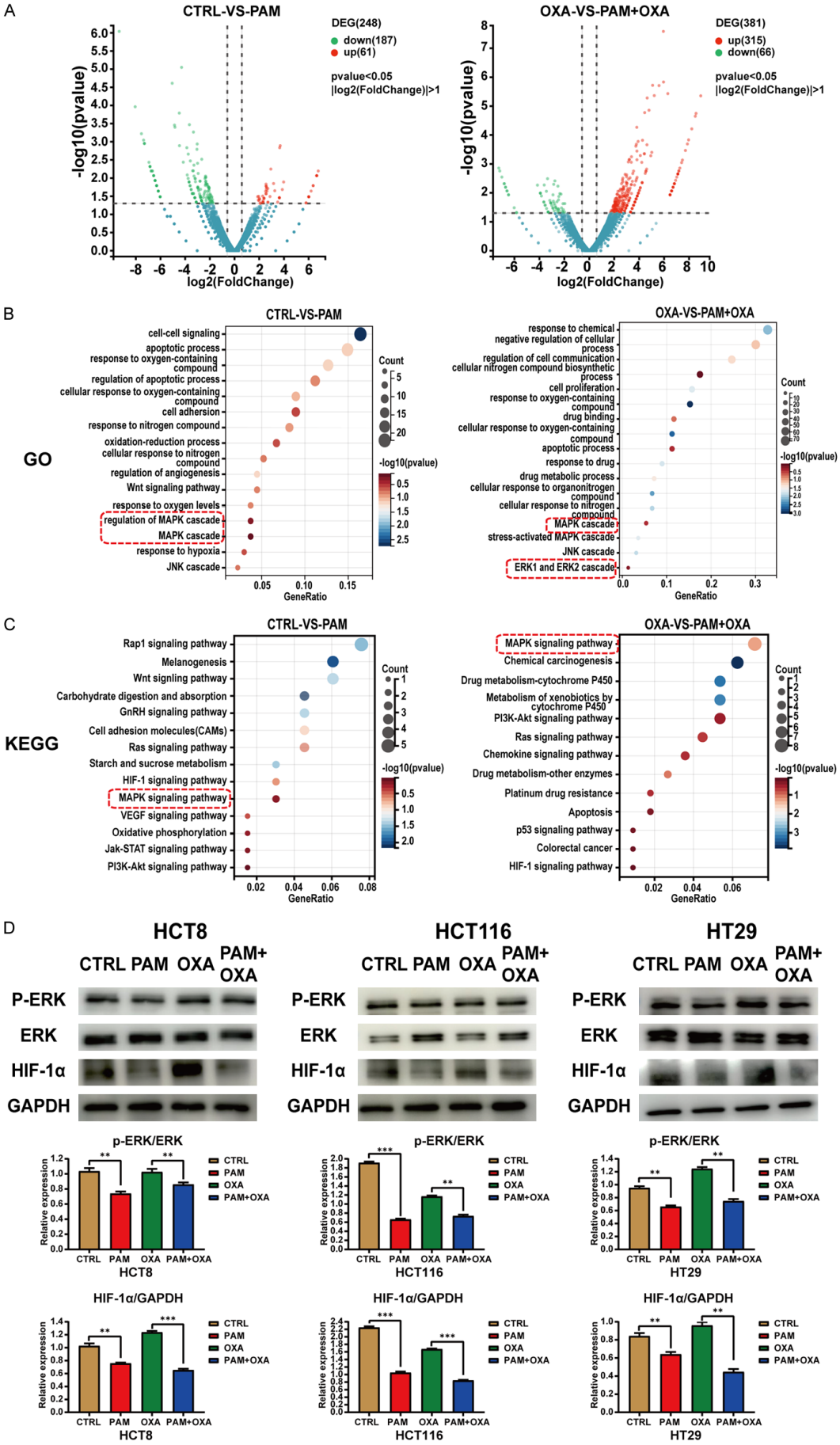
A
CTRL-VS-PAM
DEG(248)
down(187)
up(61)
pvalue<0.05
|log2(FoldChange)|>1
-log10(pvalue)
log2(FoldChange)
OXA-VS-PAM+OXA
DEG(381)
up(315)
down(66)
pvalue<0.05
|log2(FoldChange)|>1
-log10(pvalue)
log2(FoldChange)
B
GO
CTRL-VS-PAM
cell-cell signaling
apoptotic process
response to oxygen-containing compound
regulation of apoptotic process
cellular response to oxygen-containing compound
cell adhesion
response to nitrogen compound
oxidation-reduction process
cellular response to nitrogen compound
regulation of angiogenesis
Wnt signaling pathway
response to oxygen levels
regulation of MAPK cascade
MAPK cascade
response to hypoxia
JNK cascade
Count
-log10(pvalue)
GeneRatio
OXA-VS-PAM+OXA
response to chemical
negative regulation of cellular process
regulation of cell communication
cellular nitrogen compound biosynthetic process
cell proliferation
response to oxygen-containing compound
drug binding
cellular response to oxygen-containing compound
apoptotic process
response to drug
drug metabolic process
cellular response to organonitrogen compound
cellular response to nitrogen compound
MAPK cascade
stress-activated MAPK cascade
JNK cascade
ERK1 and ERK2 cascade
Count
-log10(pvalue)
GeneRatio
C
KEGG
CTRL-VS-PAM
Rap1 signaling pathway
Melanogenesis
Wnt signaling pathway
Carbohydrate digestion and absorption
GnRH signaling pathway
Cell adhesion molecules(CAMs)
Ras signaling pathway
Starch and sucrose metabolism
HIF-1 signaling pathway
MAPK signaling pathway
VEGF signaling pathway
Oxidative phosphorylation
Jak-STAT signaling pathway
PI3K-Akt signaling pathway
Count
-log10(pvalue)
GeneRatio
OXA-VS-PAM+OXA
MAPK signaling pathway
Chemical carcinogenesis
Drug metabolism-cytochrome P450
Metabolism of xenobiotics by cytochrome P450
PI3K-Akt signaling pathway
Ras signaling pathway
Chemokine signaling pathway
Drug metabolism-other enzymes
Platinum drug resistance
Apoptosis
p53 signaling pathway
Colorectal cancer
HIF-1 signaling pathway
Count
-log10(pvalue)
GeneRatio
D
HCT8
HCT116
HT29
CTRL PAM OXA PAM+ OXA
P-ERK
ERK
HIF-1α
GAPDH
p-ERK/ERK
HIF-1α/GAPDH
Relative expression
CTRL
PAM
OXA
PAM+OXA
HCT8
HCT116
HT29

Figure 6. Investigation of the potential mechanism involved in the PAM-induced HIF-1α decrease by transcriptome sequencing. (A) Volcano plot of differentially expressed genes in groups of CTRL-treated xenografts versus PAM-treated xenografts (left) and in groups of OXA-treated xenografts versus PAM+OXA-treated xenografts (right). (B) GO and (C) KEGG analysis for differentially expressed genes in (A). MAPK pathways are highlighted using red boxes. (D) The expression levels of P-ERK, ERK and HIF-1α in different xenografts were validated by western blot, and quantity analysis was performed using ImageJ software. GAPDH was used as the endogenous control. The results are presented as the mean ± standard deviation of three independent experiments. $^{*}P < 0.05$, $^{**}P < 0.01$, $^{***}P < 0.001$.

the response of cells to active substances in PAM, including response to oxygen containing compound and response to nitrogen compound. Next, the KEGG analysis of CTRL vs. PAM emphasizes changes in the HIF-1α signaling path, MAPK signaling path, and PI3K-Akt signaling path. At the same time as OXA vs. PAM+OXA changes in the above pathways, Apoptosis and p53 signaling pathways also undergo changes. Meanwhile, relevant studies have shown that PI3K-Akt and MAPK are two upstream pathways that regulate HIF-1α expression [36]. In our previous research, we found that PAM can significantly inhibit the expression of PI3K-Akt [12]. Therefore, this experiment will conduct preliminary validation in the MAPK pathway.

Compared with control or OXA treated xenografts, PAM or PAM+OXA significantly inhibited the expression of HIF-1α and phosphorylated ERK rather than total ERK. In addition, the MAPK/p38 pathway is necessary for the hypoxic activation of HIF-1α [16], and its inhibition by PAM will also lead to a decrease in HIF-1α. At the same time, some studies have found that p-p38 contributes to the drug resistance of several types of tumors to chemotherapy [17, 37]. Among them, inhibiting p-p38 in the colon cancer mouse model can enhance the effect of traditional chemotherapy (such as cisplatin, 5-FU or irinotecan) [38, 39], which also confirms that PAM can effectively improve chemotherapy sensitivity. These results suggested that PAM exerted its inhibitory effect by alleviating hypoxia, as indicated by decreased HIF-1α expression and MAPK pathway inhibition. Based on our preliminary analysis, other pathways or molecules might also be involved in hypoxia, which will be explored in detail.

In summary, this study showed that PAM could reduce hypoxia-induced HIF-1α expression in hypoxia CRC cells *in vitro* and in xenografts *in vivo* and enhance chemosensitivity by alleviating hypoxia. MAPK pathway inhibition by PAM might be the major mechanism involved in the inhibitory effect of PAM; however, detailed regulatory mechanisms need to be elucidated in the future. Our results provide a promising combination strategy for clinical application.

Acknowledgements

This study was supported by the Science, Technology, and Innovation Commission of Shenzhen Municipality (KCXFZ20200201101-050887, ZDSYS20190902092855097, GJHZ20200731095207023) and the Shenzhen Sanming Project (SZSM201612041) and supported by the National Natural Science Foundation of China (52007001).

Disclosure of conflict of interest

None.

Address correspondence to: Yajie Liu, Department of Radiation Oncology, Peking University Shenzhen Hospital, Shenzhen 518036, Guangdong, China. Tel: +86-13823394075; E-mail: Anthea1966@163.com; Jing Gao and Shubin Wang, Department of Oncology, Peking University Shenzhen Hospital, Shenzhen 518036, Guangdong, China. Tel: +86-13581565966; E-mail: gaojing_pumc@163.com (JG); Tel: +86-13823394076; E-mail: wangshubin2013@163.com (SBW)

References

[1] Siegel RL, Miller KD and Jemal A. Cancer statistics, 2020. CA Cancer J Clin 2020; 70: 7-30.

[2] Simões-Sousa S, Littler S, Thompson SL, Minshall P, Whalley H, Bakker B, Belkot K, Moralli D, Bronder D, Tighe A, Spierings DCJ, Bah N, Graham J, Nelson L, Green CM, Foijer F, Townsend PA and Taylor SS. The p38α stress Kinase suppresses aneuploidy tolerance by inhibiting Hif-1α. Cell Rep 2018; 25: 749-760, e746.

[3] Meng L, Cheng Y, Tong X, Gan S, Ding Y, Zhang Y, Wang C, Xu L, Zhu Y, Wu J, Hu Y and Yuan A. Tumor oxygenation and hypoxia inducible factor-1 functional inhibition via a reactive oxygen species responsive nanoplatform for enhancing radiation therapy and abscopal effects. ACS Nano 2018; 12: 8308-8322.

[4] Luo Z, Tian H, Liu L, Chen Z, Liang R, Chen Z, Wu Z, Ma A, Zheng M and Cai L. Tumor-targeted hybrid protein oxygen carrier to simultaneously enhance hypoxia-dampened chemotherapy and photodynamic therapy at a single dose. Theranostics 2018; 8: 3584-3596.
[5] Ortmann B, Druker J and Rocha S. Cell cycle progression in response to oxygen levels. Cell Mol Life Sci 2014; 71: 3569-3582.
[6] Xu K, Zhan Y, Yuan Z, Qiu Y, Wang H, Fan G, Wang J, Li W, Cao Y, Shen X, Zhang J, Liang X and Yin P. Hypoxia induces drug resistance in colorectal cancer through the HIF-1α/miR-338-5p/IL-6 feedback loop. Mol Ther 2019; 27: 1810-1824.
[7] Rashid M, Zadeh LR, Baradaran B, Molavi O, Ghesmati Z, Sabzichi M and Ramezani F. Up-down regulation of HIF-1alpha in cancer progression. Gene 2021; 798: 145796.
[8] Minassian LM, Cotechini T, Huitema E and Graham CH. Hypoxia-induced resistance to chemotherapy in cancer. Adv Exp Med Biol 2019; 1136: 123-139.
[9] Prieto-Vila M, Takahashi RU, Usuba W, Kohama I and Ochiya T. Drug resistance driven by cancer stem cells and their Niche. Int J Mol Sci 2017; 18: 2574.
[10] Yan X, Ouyang J, Zhang C, Shi Z, Wang B and Ostrikov KK. Plasma medicine for neuroscience-an introduction. Chin Neurosurg J 2019; 5: 25.
[11] Motaln H, Recek N and Rogelj B. Intracellular responses triggered by cold atmospheric plasma and plasma-activated media in cancer cells. Molecules 2021; 26: 1336.
[12] Li Y, Lv Y, Zhu Y, Yang X, Lin B, Li M, Zhou Y, Tan Z, Choi EH, Wang J, Wang S and Liu Y. Low-temperature plasma-activated medium inhibited proliferation and progression of lung cancer by targeting the PI3K/Akt and MAPK pathways. Oxid Med Cell Longev 2022; 2022: 9014501.
[13] Li Y, Lv Y, Tang M, Choi EH, Wang J, Lv G, Zhu Y, Wang S and Liu Y. Low-temperature plasma-jet-activated medium inhibited tumorigenesis of lung adenocarcinoma in a 3D in vitro culture model. Plasma Process Polym 2021; 18: e2100049.1-e2100049.14.
[14] Li W, Yu H, Ding D, Chen Z, Wang Y, Wang S, Li X, Keidar M and Zhang W. Cold atmospheric plasma and iron oxide-based magnetic nanoparticles for synergetic lung cancer therapy. Free Radic Biol Med 2019; 130: 71-81.
[15] Salaroglio IC, Mungo E, Gazzano E, Kopecka J and Riganti C. ERK is a pivotal player of chemo-immune-resistance in cancer. Int J Mol Sci 2019; 20: 2505.
[16] Corre I, Paris F and Huot J. The p38 pathway, a major pleiotropic cascade that transduces stress and metastatic signals in endothelial cells. Oncotarget 2017; 8: 55684-55714.
[17] García-Cano J, Roche O, Cimas FJ, Pascual-Serra R, Ortega-Muelas M, Fernández-Aroca DM and Sánchez-Prieto R. p38MAPK and chemotherapy: we always need to hear both sides of the story. Front Cell Dev Biol 2016; 4: 69.
[18] Wang Y, Bai C, Ruan Y, Liu M, Chu Q, Qiu L, Yang C and Li B. Coordinative metabolism of glutamine carbon and nitrogen in proliferating cancer cells under hypoxia. Nat Commun 2019; 10: 201.
[19] Zhang B, Li SL, Xie HL, Fan JW, Gu CW, Kang C and Teng MJ. Effects of silencing the DUSP1 gene using lentiviral vector-mediated siRNA on the release of proinflammatory cytokines through regulation of the MAPK signaling pathway in mice with acute pancreatitis. Int J Mol Med 2018; 41: 2213-2224.
[20] Feng Y, Sakamoto N, Wu R, Liu JY, Wiese A, Green ME, Green M, Akyol A, Roy BC, Zhai Y, Cho KR and Fearon ER. Tissue-specific effects of reduced beta-catenin expression on adenomatous polyposis coli mutation-instigated tumorigenesis in mouse colon and ovarian epithelium. PLoS Genet 2015; 11: e1005638.
[21] Sahores A, May M, Sequeira GR, Fuentes C, Jacobsen B, Lanari C and Lamb CA. Targeting FGFR with BGJ398 in breast cancer: effect on tumor growth and metastasis. Curr Cancer Drug Targets 2018; 18: 979-987.
[22] Sun Y, Xing X, Liu Q, Wang Z, Xin Y, Zhang P, Hu C and Liu Y. Hypoxia-induced autophagy reduces radiosensitivity by the HIF-1alpha/miR-210/Bcl-2 pathway in colon cancer cells. Int J Oncol 2015; 46: 750-756.
[23] Yong Y, Zhang C, Gu Z, Du J, Guo Z, Dong X, Xie J, Zhang G, Liu X and Zhao Y. Polyoxometalate-based radiosensitization platform for treating hypoxic tumors by attenuating radioresistance and enhancing radiation response. ACS Nano 2017; 11: 7164-7176.
[24] Poljakova J, Groh T, Gudino ZO, Hrabeta J, Borek-Dohalska L, Kizek R, Doktorova H, Eckschlager T and Stiborova M. Hypoxia-mediated histone acetylation and expression of N-myc transcription factor dictate aggressiveness of neuroblastoma cells. Oncol Rep 2014; 31: 1928-1934.
[25] Song S, Park JT, Na JY, Park MS, Lee JK, Lee MC and Kim HS. Early expressions of hypoxia-inducible factor 1alpha and vascular endothelial growth factor increase the neuronal plasticity of activated endogenous neural stem cells after focal cerebral ischemia. Neural Regen Res 2014; 9: 912-918.
[26] Yoshimura H, Dhar DK, Kohno H, Kubota H, Fujii T, Ueda S, Kinugasa S, Tachibana M and Nagasue N. Prognostic impact of hypoxia-in-

ducible factors 1α and 2α in colorectal cancer patients: correlation with tumor angiogenesis and cyclooxygenase-2 expression. Clin Cancer Res 2004; 10: 8554-8560.
[27] Xu R, Wang W, Zhu B, Lin X, Ma D, Zhu L, Zhao Q, Nie Y, Cai X, Li Q, Fang W, Li H, Wang N, Chen Y, Peng C, Fang H and Shen L. Disease characteristics and treatment patterns of Chinese patients with metastatic colorectal cancer: a retrospective study using medical records from China. BMC Cancer 2020; 20: 131.
[28] Feil L, Koch A, Utz R, Ackermann M, Barz J, Stope M, Kramer B, Wallwiener D, Brucker SY and Weiss M. Cancer-selective treatment of cancerous and non-cancerous human cervical cell models by a non-thermally operated electrosurgical argon plasma device. Cancers (Basel) 2020; 12: 1037.
[29] Gumbel D, Bekeschus S, Gelbrich N, Napp M, Ekkernkamp A, Kramer A and Stope MB. Cold atmospheric plasma in the treatment of osteosarcoma. Int J Mol Sci 2017; 18: 2004.
[30] Bauer G. Targeting protective catalase of tumor cells with cold atmospheric plasma-activated medium (PAM). Anticancer Agents Med Chem 2018; 18: 784-804.
[31] Gonzalez N, Cardama GA, Comin MJ, Segatori VI, Pifano M, Alonso DF, Gomez DE and Menna PL. Pharmacological inhibition of Rac1-PAK1 axis restores tamoxifen sensitivity in human resistant breast cancer cells. Cell Signal 2017; 30: 154-161.
[32] Chicote I, Camara JA and Palmer HG. Advanced colorectal cancer orthotopic patient-derived xenograft models for cancer and stem cell research. Methods Mol Biol 2020; 2171: 321-329.
[33] Burgenske DM, Monsma DJ and MacKeigan JP. Patient-derived xenograft models of colorectal cancer: procedures for engraftment and propagation. Methods Mol Biol 2018; 1765: 307-314.
[34] Kawczyk-Krupka A, Bugaj AM, Latos W, Zaremba K, Wawrzyniec K, Kucharzewski M and Sieron A. Photodynamic therapy in colorectal cancer treatment--the state of the art in preclinical research. Photodiagnosis Photodyn Ther 2016; 13: 158-174.
[35] Nompumelelo Simelane NW, Kruger CA and Abrahamse H. Photodynamic diagnosis and photodynamic therapy of colorectal cancer in vitro and in vivo. RSC Adv 2020; 10: 41560-41576.
[36] Masoud GN and Li W. HIF-1α pathway: role, regulation and intervention for cancer therapy. Acta Pharm Sin B 2015; 5: 378-389.
[37] Liu F, Gore AJ, Wilson JL and Korc M. DUSP1 is a novel target for enhancing pancreatic cancer cell sensitivity to gemcitabine. PLoS One 2014; 9: e84982.
[38] Igea A and Nebreda AR. The stress kinase p38α as a target for cancer therapy. Cancer Res 2015; 75: 3997-4002.
[39] Rudalska R, Dauch D, Longerich T, McJunkin K, Wuestefeld T, Kang TW, Hohmeyer A, Pesic M, Leibold J, von Thun A, Schirmacher P, Zuber J, Weiss KH, Powers S, Malek NP, Eilers M, Sipos B, Lowe SW, Geffers R, Laufer S and Zender L. In vivo RNAi screening identifies a mechanism of sorafenib resistance in liver cancer. Nat Med 2014; 20: 1138-1146.

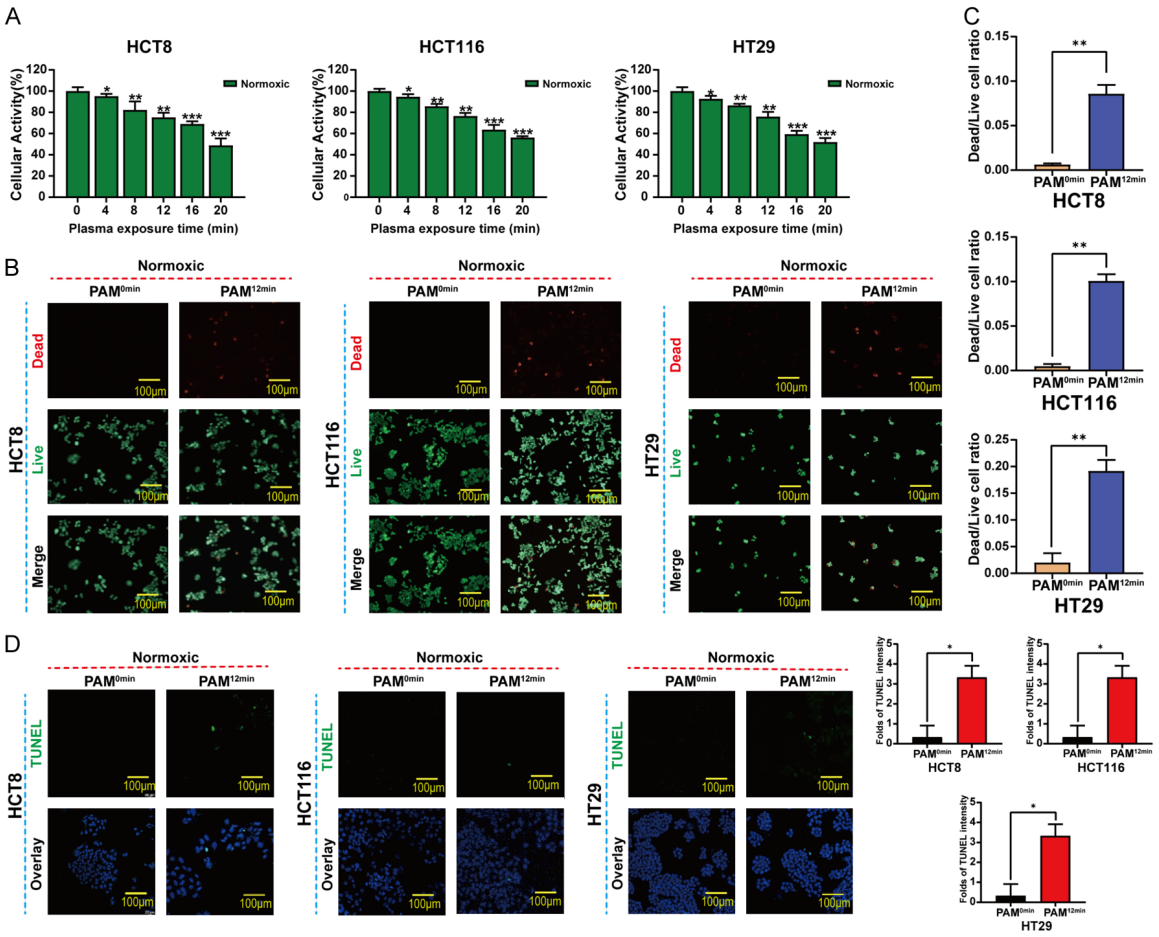

Figure S1. PAM inhibits the activity of normoxic CRC cells. A. Normoxic CRC cells could be inhibited by PAM in a plasma exposure time dependent manner. B. The staining results of live/dead cells treated with or without PAM. Red represented dead cells and green represented live cells. C. The quantification of dead/live cell ratio in CRC cells treated with or without PAM. D. The percentage of cell apoptosis was increased by PAM in normoxic CRC cells evaluated by TUNEL assay. Results are presented as mean ± standard deviation of three independent experiments. $^{*}P < 0.05$, $^{**}P < 0.01$, $^{***}P < 0.001$.

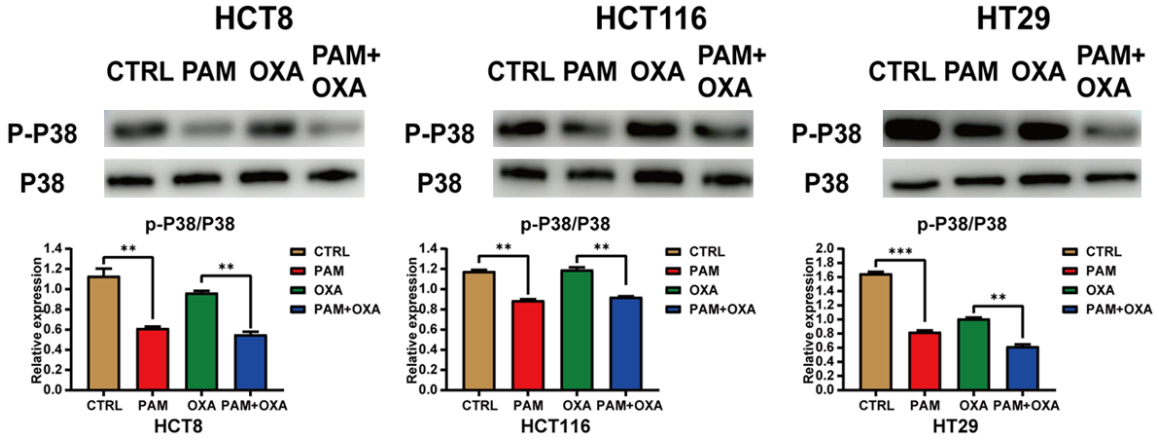

Figure S2. PAM inhibits phosphorylation of P38. Results are presented as mean ± standard deviation of three independent experiments. $^{*}P < 0.05$, $^{**}P < 0.01$, $^{***}P < 0.001$.